

# We are IntechOpen, the world's leading publisher of Open Access books Built by scientists, for scientists

6,900

Open access books available

185,000

International authors and editors

200M

Downloads

Our authors are among the

154

Countries delivered to

TOP 1%

most cited scientists

12.2%

Contributors from top 500 universities



WEB OF SCIENCE™

Selection of our books indexed in the Book Citation Index  
in Web of Science™ Core Collection (BKCI)

Interested in publishing with us?  
Contact [book.department@intechopen.com](mailto:book.department@intechopen.com)

Numbers displayed above are based on latest data collected.  
For more information visit [www.intechopen.com](http://www.intechopen.com)



# Water Splitting Technologies for Hydrogen Cogeneration from Nuclear Energy

Zhaolin Wang and Greg F. Naterer

*Clean Energy Research Laboratory, Faculty of Engineering and Applied Science,  
University of Ontario Institute of Technology (UOIT), Ontario,  
Canada*

## 1. Introduction

Currently, nuclear energy is mainly utilized for the generation of electricity that is distributed to end users via power transmission networks. However, there are also other distribution forms. For example, hydrogen produced from nuclear energy is a promising future energy carrier that can be delivered to end users for purposes of heating homes, fuel supply for hydrogen vehicles and other residential applications, while simultaneously lowering the greenhouse gas emissions of otherwise using fossil fuels [Forsberg, 2002, 2007]. Current industrial demand for hydrogen exists in the upgrading of heavy oils such as oil sands, refineries, fertilizers, automotive fuels, and manufacturing applications among others. Hydrogen production is currently a large, rapidly growing and profitable industry. The worldwide hydrogen market is currently estimated at about \$300 billion per year, growing at about 10% per year, growing to 40% per year by 2020 and expected to reach several trillions of dollars per year by 2020 [Naterer et al., 2008]. This chapter will examine the usage of nuclear energy for the cogeneration of electricity and hydrogen with water splitting technologies.

In section 2 of this chapter, various hydrogen production methods will be briefly introduced and compared. The potential economics and reduction of greenhouse gas emissions with nuclear hydrogen production are examined. In section 3, matching the heat requirements of various thermochemical hydrogen cycles to the available heat from nuclear reactors (especially Generation IV) will be studied from the aspects of heat grade, magnitude, and distribution inside the cycles. The requirement of an intermediate heat exchanger between the nuclear reactor and hydrogen production plant is discussed. Long distance heat transport is examined from the aspects of the performance of working fluids, flow characteristics, and heat losses in the transport pipeline. In section 4, layout options for the integration of nuclear reactors and hydrogen production plants are discussed. In section 5, modulations of nuclear energy output and hydrogen cogeneration scales are studied, regarding the increase of the nuclear energy portion on the power grid through the adjustment of the hydrogen production rate so as to lower the needs for fossil fuels. The options for keeping the total nuclear energy output at a constant value and simultaneously varying the electricity output onto the power grid in order to approach a load following profile for peak and off-peak hours are discussed. In section 6, conclusions are provided for the cogeneration of hydrogen with nuclear heat.

2. Environmental and economic benefits of nuclear hydrogen production methods

The growing demand for hydrogen will have a significant impact on the economy. However, currently the major production methods for hydrogen are not clean, although its usage is clean. More than 95% of the global hydrogen is directly produced from fossil fuels, i.e., about 48% from steam methane reforming (SMR), 30% from refinery/chemical off-gases, and 18% from coal gasification [NYSERDA , 2010; IEA, 2010]. Water electrolysis accounts for less than 4%, and even this 4% is not “clean” because the electricity used is not fully generated from clean sources. The usage of fossil fuels to produce hydrogen has been resulting in major greenhouse gas emissions and other hazardous pollutants. Table 1 shows the CO<sub>2</sub> emission levels of various production methods [Wang et al., 2010]. On average, the CO<sub>2</sub> emissions are 19 tonnes per tonne of hydrogen production, which results in 959 million tonnes of CO<sub>2</sub> emissions per annum. Therefore, the future hydrogen economy must be based on clean production technologies.

Scientists and engineers have been attempting for years to develop new technologies for clean and efficient hydrogen production. Among the technologies, photoelectrochemical water splitting, water electrolysis with off-peak hours electricity, high temperature electrolysis (HTE), and thermochemical water splitting are promising clean options. To evaluate these options, the clean extent of the energy source, thermal efficiency and economics are the three major criteria. In terms of the clean extent, photoelectrochemical water splitting utilizes sunlight to split water into hydrogen and oxygen [Sivula et al., 2010]. However, due to the intermittent nature of sunlight, this production method cannot deliver a continuous flow of hydrogen production at night and other times when sunlight is not available. Water electrolysis can utilize off-peak hour electricity from the power grid that can improve the hydrogen production economics, due to the lower price of electricity at off-peak hours. However, it may not be clean production because the power sources contributing to the power grid are not fully clean. As shown in Table 1, water electrolysis cannot even provide a better scenario than steam methane reforming and coal gasification if using the existing power grid. To make the water electrolysis “clean”, the electricity must be derived from a clean source. Regarding high temperature electrolysis and thermochemical water splitting methods that utilize some heat as a portion of energy input, the same situation exists because the heat must also be derived from clean sources so as to deliver a clean production method. Solar, wind, and nuclear energy are sustainable options for energy sources [Steinfeld, 2005; Schultz et al., 2003; Kreith et al., 2007]. Among these options, nuclear energy is more mature and widespread than solar and wind in current industry. Overcoming the intermittency of solar and wind energy is a long-term challenging task. Therefore, to integrate nuclear power with hydrogen production is a promising option.

| Method   | SMR  | Coal gasification | Water electrolysis  |
|--|------|-------------------|---------------------|
| CO <sub>2</sub> emissions <sup>(a)</sup><br>CO <sub>2</sub> /H <sub>2</sub> (Moles/mole)   | 0.51 | 1.21              | 1.00 <sup>(b)</sup> |
| (a) Heat from fossil fuel combustion and electricity from the existing power grid.<br>(b) 84% of the electricity from fossil power generation (Alberta, Canada [Government of Alberta, 2008]). |      |                   |                     |

Table 1. CO<sub>2</sub> emissions with current production methods and energy sources

In terms of production efficiency, the thermal efficiency of a hydrogen production cycle can be defined as follows:

$$\varepsilon = \frac{\Delta H_f}{\Delta H_{\text{NetInput}} + \Delta E_{\text{Electrolysis}}} \times 100\% \quad (1)$$

where  $\Delta H_f$  is the formation enthalpy of water with the value of 286 kJ/mol  $\text{H}_2\text{O}$ ,  $\Delta E_{\text{Electrolysis}}$  is the electrical energy required for the process of electrolysis, and  $\Delta H_{\text{NetInput}}$  is the net heat input to the cycle. Equation (1) can apply to conventional electrolysis, high temperature electrolysis, and thermochemical (either fully thermal or hybrid) water splitting cycles. If the value of  $\Delta H_{\text{NetInput}}$  is zero, then it indicates pure electrolysis. Conversely, if  $\Delta E_{\text{electrolysis}}$  is zero, it means a purely thermal water splitting process that only uses heat. If neither is zero, it is a hybrid process. The power generation process can be subdivided into three stages: (1) heat is generated from a nuclear reactor; (2) heat converts to mechanical energy by driving a steam or gas turbine, which makes an electric generator rotate; (3) rotation of electric generator produces AC electric power. Each stage inevitably experiences some heat loss. To produce hydrogen from conventional water electrolysis, all three stages are experienced, plus an additional stage of converting AC to DC. Therefore, although the conversion efficiency from DC electrical to chemical energy in a water electrolyzer could reach 80~90% [Forsberg, 2002, 2003], the overall thermal efficiency is only around 30%. The power generation efficiency of future nuclear reactors will be increased significantly, e.g., utilizing Generation IV nuclear reactors [WNA, 2010].

In terms of the economics of various hydrogen production methods, lower costs lead to better economics. In this chapter, the word “cost” is discussed in terms of monetary spending per unit of hydrogen, e.g., US\$/tonne  $\text{H}_2$ , in order to avoid confusion with the term “efficiency” because “cost” is often used interchangeably in place of efficiency in cost-effectiveness analyses and efficiency assessments.

Table 2 lists the thermal efficiencies and costs of various hydrogen production methods with nuclear energy on a comparative basis. Detailed thermal efficiency calculations and cost analyses were reported in past studies [Wang et al., 2010; Jean-Pierre Py et al., 2006; de Jong et al., 2009; Kreith et al., 2007]. In Table 2, the cost of steam methane reforming that utilizes the combustion heat of methane is also shown for a comparison since it is today’s major production method. The S-I and Cu-Cl cycles are selected as typical thermochemical hydrogen production cycles that will be studied in subsequent sections. It can be found that the costs of various hydrogen production technologies with nuclear energy are similar to that of steam methane reforming, especially, thermochemical cycles integrated with Generation IV nuclear reactors, e.g., supercritical water-cooled reactor (SCWR). The cycles have the potential to deliver lower production costs than other methods.

Regarding the  $\text{CO}_2$  emissions of thermochemical cycles, as discussed previously, a hybrid cycle utilizes a portion of electricity for its electrolytic step. If the electricity is not derived from non-fossil fuel sources, then  $\text{CO}_2$  emissions will be generated. Table 3 shows the emission comparison for the current power grid and nuclear power plant. According to the structure of energy sources on the power grid, the emissions were estimated [Wang et al., 2010]. Comparing Tables 3 and 1, it can be observed that hydrogen production with thermochemical cycles and nuclear energy can lower the  $\text{CO}_2$  emissions by at least one order, regardless of the energy sources for electricity.

| <div>Production</div> <div>Condition</div>   | Thermochemical |             | HTE                | Electrolysis | SMR                    |
|--|----------------|-------------|--------------------|--------------|------------------------|
|  | S-I cycle      | Cu-Cl cycle |                    |              |                        |
| pricing year   | 2003           | 2003        | 2003               | 2003         | 2003                   |
| Nuclear reactor  | VHTR           | SCWR        | GenIV              | GenIII+      | methane <sup>(a)</sup> |
| T, °C  | 950            | 650         | 800                | 650          | 700-- 1100             |
| Price ratio<br>$E_{\text{electricity}}/E_{\text{heat}}$  | 3              | 3           | 3                  | 3            | 3                      |
| production efficiency  | 52%            | 52%         | 52%                | 41%          | 65~75%                 |
| ratio (capital recovery /<br>operating cost)   | 0.77           | 0.40        | N/A <sup>(b)</sup> | 0.32         | 0.46                   |
| production scale<br>(tonnes H <sub>2</sub> / day)  | 200            | 200         | 208                |              | 200                    |
|  |                | (10)        |                    | 10           |                        |
| Cost, US \$/ kgH <sub>2</sub>  | 1.85           | 1.60        | 2.25               |              |                        |
|  |                | (2.31)      |                    | 2.52         | 2.67                   |
| <div>Note:</div> <div>(a) Current SMR uses the combustion heat of methane.</div> <div>(b) Not reported in literatures for industrial scale hydrogen production.</div> <div>Acronyms of nuclear reactors:</div> <div>GenIII+ (Advanced Generation III reactor), GenIV (Generation IV nuclear reactor), SCWR (Supercritical water reactor), VHTR (Very high temperature reactor).</div> <div>Acronyms of hydrogen production methods:</div> <div>Cu-Cl cycle (copper-chlorine thermochemical cycle), HTE (high temperature electrolysis), S-I cycle (sulfur-iodine thermochemical cycle), SMR (steam methane reforming).</div> |                |             |                    |              |                        |

Table 2. Costs of various nuclear powered hydrogen production methods.

| Thermochemical cycle  | S-I, fully thermal <sup>(a)</sup> | Cu-Cl, hybrid |                     |
|---|-----------------------------------|---------------|---------------------|
| CO <sub>2</sub> emissions, CO <sub>2</sub> /H <sub>2</sub> (Moles /mole)  | 0                                 | 0             | 0.07 <sup>(b)</sup> |
| <div>(a) Energy source for electricity generation has no influence on CO<sub>2</sub> emssions.</div> <div>(b) 84% of the electricity from fossil power generation [Government of Alberta, 2008]).</div> |                                   |               |                     |

Table 3. CO<sub>2</sub> emissions with nuclear powered thermochemical production methods

3. Thermal integration of thermochemical cycles and nuclear reactors

3.1 Matching the temperatures of thermochemical cycles and nuclear reactors

Many thermochemical hydrogen production cycles have been developed to split water thermally through auxiliary chemical compounds and reactions. About two hundred thermochemical cycles were reported to produce hydrogen by thermochemical water splitting [Sadhankar et al., 2005; Forsberg, 2003]. Different cycles have various inputs of temperatures that must be provided by nuclear reactors. Table 4 shows the temperatures of some thermochemical cycles and nuclear reactors. Among these cycles, the sulfur-iodine (S-I) cycle is a leading example of purely thermal cycles that has been scaled up from proof-of-principle tests to a large engineering scale by the Japan Atomic Energy Agency (JAEA,

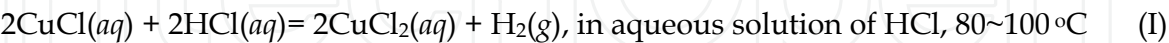
[Kubo et al., 2004]). Among the hybrid thermal cycles, the copper-chlorine (Cu-Cl) cycle is a leading example and its scale-up is underway at the University of Ontario Institute of Technology [Wang et al., 2010] in collaboration with its partners that include Atomic Energy of Canada Limited (AECL). The maximum temperature required by thermochemical cycles can be met by Generation IV nuclear reactors. The temperature requirement of the Cu-Cl cycle is much lower than that of other cycles. Therefore, the Cu-Cl cycle can more readily link with the heat output of various nuclear reactors due to its lower temperature requirement.

| Cycle name   | T, °C | Development status |
|--|-------|--------------------|
| MSO <sub>4</sub> -NH <sub>3</sub> (metal sulphate – ammonia) cycles<br>M: Zn, Mg, Ca, Ba, Fe, Co, Ni, Mn, Cu | 1,100 | Proof-of-principle |
| Mn-C (carbon dioxide – Manganese oxide) cycle  | 977   | Proof-of-principle |
| Mn-Cl (manganese – chlorine) cycle   | 900   | Proof-of-principle |
| S-Br (sulfur - bromine), Cr-Cl (chromium - chlorine),<br>and V-Cl (vanadium – chlorine) cycles               | 850   | Proof-of-principle |
| S-I (sulphur - iodine) cycle   | 850   | Under scale-up     |
| Ni-Fe (nickel – ferrite) cycle   | 800   | Proof-of-principle |
| Mn-Na (manganese - sodium) cycle   | 800   | Proof-of-principle |
| Fe-Ca-Br (ferrite-calcium-bromine) cycle   | 750   | Proof-of-principle |
| Fe-Cl (ferrite – chlorine) cycle   | 650   | Proof-of-principle |
| Hg-HgO (mercury – mercury oxide) cycle   | 600   | Proof-of-principle |
| Cu-Cl (copper - chlorine) cycle  | 530   | Under scale-up     |
|  |       |                    |
| Reactors   | T, °C | Development status |
| Generations II and III   | <450  | Commercialized     |
| Generations III+ and IV  | >450  | Under development  |

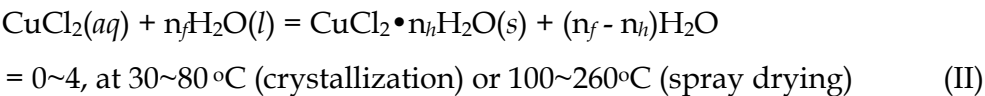
Table 4. Temperatures of thermochemical cycles and nuclear reactors

There are several types of Cu-Cl cycles with various numbers of steps from 2 to 5 depending on reaction conditions. Due to the lower efficiency and more engineering challenges of two-, three- and five-step cycles, the following cycle with 4 steps will be considered in this chapter [Wang et al., 2009]:

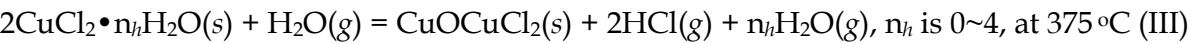
**Step 1.** Hydrogen production step (electrolysis)



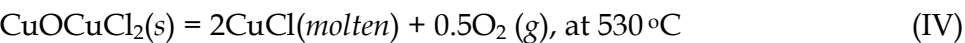
**Step 2.** Drying step (endothermic)



**Step 3.** Hydrolysis step (endothermic)



**Step 4.** Oxygen production step (endothermic)



3.2 Matching the nuclear heat and hydrogen production requirements

Even if the temperature of a nuclear reactor can reach the maximum temperature requirement of 530°C, it may not match the heat distribution that is regulated by different temperatures at different steps. Table 5 shows the heat requirements of the Cu-Cl cycle [Wang et al., 2009]. It can be found that different steps occupy different heat percentages. If the heat source does not match the required distribution, then one or two steps may not be supplied with sufficient heat and simultaneously another one or two steps may be supplied with surplus heat. Therefore, the temperature of the heat source should cover the maximum temperature requirement of the Cu-Cl cycle, as well as provide a similar heat requirement structure.

| Step  | T, °C | Net heat input <sup>(a)</sup><br>kJ/mol H <sub>2</sub> | Compared with the total<br>net heat input, % |
|---|-------|--|--|
| I   | <100  | 0  | 0%   |
| II  | <200  | 122.2  | 26.9%  |
| III   | ≥375  | 181.8  | 40.1%  |
| IV  | ≥530  | 149.4  | 33.0%  |
| Sum <sup>(b)</sup>  |       | 453.4 (226.7MJ/kg H <sub>2</sub> )                     | 100%   |
| (a) 50% of the heat released by exothermic processes of Cu-Cl cycle is recovered. |       |  |  |
| (b) The sum includes all unlisted auxiliary processes for each step.              |       |  |  |

Table 5. Heat requirements of the Cu-Cl cycle

The distribution of heat inputs depends on the temperatures of the working fluid, i.e., heat transfer fluid, entering and exiting the Cu-Cl cycle. The nuclear heat must be transported over a distance through a heat transfer fluid to the thermochemical hydrogen production plant. Due to the design and operation complexity of dealing with phase change heat transfer fluids, only sensible heat is considered in this chapter for the heating purposes of the Cu-Cl cycle. In this chapter, 250°C is selected as the maximum temperature of heat transfer fluid exiting the Cu-Cl cycle, which is about 100°C lower than most of the inlet temperatures of Generation IV nuclear reactors, so as to have a sufficient temperature difference for heat exchange between the heat transfer fluid and the nuclear reactor coolants. Later sections of this paper will discuss further details of the temperature selection criteria based on the calculations of heat losses. Since only sensible heat of the heat transfer fluid is provided to the Cu-Cl cycle, the delivered heat requirement of the heat transfer fluid can be estimated by variations of the fluid temperature passing through each step of the Cu-Cl cycle, assuming the heat capacity of the heat transfer fluid does not vary significantly in the temperature range of interest. The matching criterion is that higher grade heat should be met at a higher priority since lower grade heat may be met by the exiting heat of higher grade steps.

Figure 1 shows the matching extent for various maximum delivered temperatures of the heat source. It can be found that 600°C can cover the maximum temperature requirement 530°C of step IV of the Cu-Cl cycle, but it does not have a sufficient heat percentage for step IV, yet it provides surplus heat for steps 2 and 1. To satisfy the heat requirement of step IV, the mass flow rate of heat transfer fluid must be increased. However, this may also deliver surplus heat to other steps. As a result, the temperature exiting the Cu-Cl cycle will be

increased and the overall thermal efficiency of both nuclear and hydrogen production plants is hence decreased. Therefore, to increase the temperature entering the Cu-Cl cycle could be a better option for satisfying the requirement. Figure 1 shows that the temperature of the heat from the nuclear reactor entering the Cu-Cl cycle after a distant transport must be around 650°C to match the heat requirements of the Cu-Cl cycle. In addition, the temperature of heat transfer fluid leaving the nuclear reactor should be sufficiently high to offset the heat losses in the transport pipeline between the nuclear and hydrogen production plants, and also to avoid condensation or solidification on the inner wall of pipeline after leaving the Cu-Cl cycle if the heat transfer fluid is steam or molten salt. An intermediate heat exchanger that can heat a transfer fluid by the nuclear reactor coolant is suggested for the heat supply to the hydrogen production plant due to the safety considerations of both the nuclear reactor and hydrogen production plant, because the nuclear reactor coolant has a risk to be contaminated by the chemicals of the Cu-Cl cycle if there is any leak in the pipe.

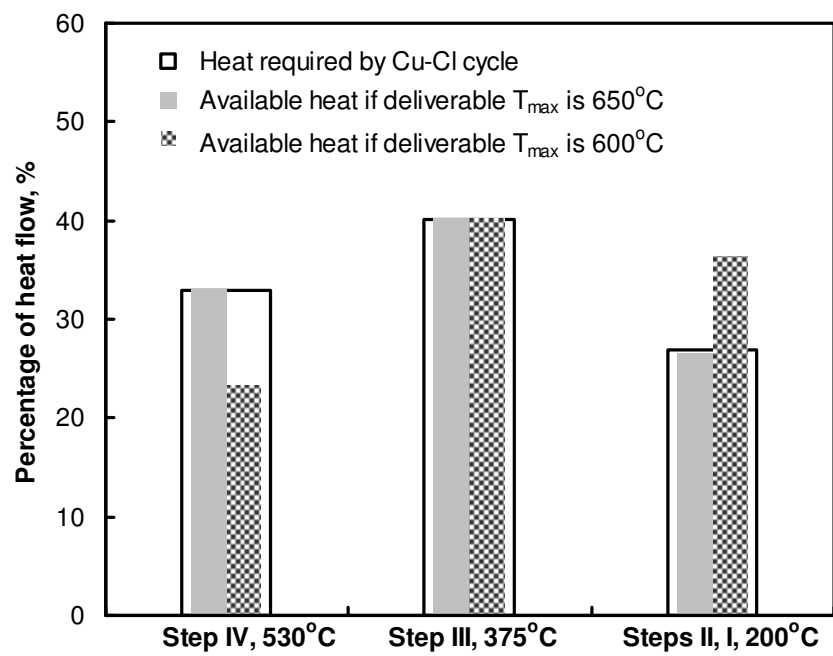


Fig. 1. Heat distribution of Cu-Cl cycle and nuclear heat source at various temperatures

3.3 Evaluation and selection of heat transfer fluids for heat transport in pipeline

Heat must be transferred by a heat transfer fluid flowing in a pipeline and transported from a nuclear power station to a thermochemical hydrogen plant. On the basis of the heat requirement per kilogram of hydrogen production shown in Table 5, the heat load can be estimated according to the hydrogen production scale. Table 6 shows the estimate, where  $Q_T$  is the heat load in the pipeline in units of  $MW_{th}$ , i.e., megawatts of thermal energy. When using sensible heat of the heat transfer fluid, the performance of the fluid can be evaluated by the required flow rate for per unit heat quantity transported in the pipeline:

$$X_T = \frac{Q_T}{\int_{T_L}^{T_H} C_p dT} \text{ at } Q_T = 1 \text{ MW}_{th}$$

(6)

where  $X_T$  has the units of  $\text{kg}\cdot\text{s}^{-1}/\text{MW}_{\text{th}}$ , and  $T_L$  and  $T_H$  are the inlet and outlet temperatures of the heat transfer fluid that extracts heat from nuclear reactor coolant in the intermediate heat exchanger. The values of  $T_L$  and  $T_H$  should prevent phase change and at the same time allow a portion of heat losses in the transport pipeline. Also,  $C_P$  is the heat capacity of the heat transfer fluid that could be thermal oils, molten salts, supercritical water, steam, or helium. To transport supercritical water, the transport pipeline must withstand a high pressure ( $>22\text{MPa}$ ), which is an engineering challenge for pipeline manufacturing and maintenance. Thermal oil may experience coking and decomposition at a high temperature. Solidification may occur in molten salt at low temperature spots. Steam may condense after a distance of transport if the pressure is higher than its saturation point. The condensation of steam indicates the need for an intermediate steam generator and two-phase flow in the transport pipeline. This may significantly increase the construction capital and operating cost. Therefore, in this chapter, the pressure of the steam is not suggested to be sufficiently high such that the steam can remain in a gaseous state during circulation.

|   |     |     |      |
|---|-----|-----|------|
| <b>H<sub>2</sub> production scale, tonnes/day</b>                       | 100 | 200 | 400  |
| <b>Heat requirement by Cu-Cl cycle , MW<sub>th</sub></b>                | 263 | 525 | 1050 |
| <b>Heat transport load (Q<sub>T</sub>) in pipeline, MW<sub>th</sub></b> | 316 | 630 | 1260 |

Table 6. Heat requirement and heat load in pipeline for various hydrogen production scales

Since step II of the Cu-Cl cycle has a temperature range of 80 - 200°C, it is assumed the heating fluid exiting the step is 230°C. To avoid condensation, the pressure of the heating fluid is 2 MPa, which is slightly lower than the saturation pressure of steam in case steam serves as the heating fluid. For a comparable study, helium is designed to have the same temperature and pressure as steam. Table 7 gives the values of  $X_T$ , the suggested operating parameters for the heat transfer fluids (helium, superheated steam, and molten salt), and the thermodynamic properties of the fluids [Petersen, 1970; Wang, 2010]. Among the three fluids of Table 7, both steam and molten salt have a phase change issue in the transport pipeline, and molten salt has an issue of chemical stability when the temperature is high. Therefore, helium is a comparatively good option for working as the heat transfer fluid.

| Fluid in pipeline          |                        | Thermodynamic properties <sup>(a)</sup> |                           |                        |            | $X_T$<br>kg s <sup>-1</sup> /MW <sub>th</sub> |
|----------------------------|------------------------|---|---------------------------|------------------------|------------|---|
|                            |                        | P<br>MPa                                | C <sub>p</sub><br>kJ/kg·K | ρ<br>kg/m <sup>3</sup> | k<br>w/m·K |   |
| Helium                     | T <sub>L</sub> = 230°C | 2                                       | 5.196                     | 1.916                  | 0.238      | 0.520   |
|                            | T <sub>H</sub> = 600°C | 2                                       | 5.196                     | 1.100                  | 0.330      |   |
| Steam                      | T <sub>L</sub> = 230°C | 2                                       | 2.735                     | 9.495                  | 0.042      | 1.189   |
|                            | T <sub>H</sub> = 600°C | 2                                       | 2.247                     | 5.010                  | 0.081      |   |
| Molten salt <sup>(b)</sup> | 230 -- 600°C           | 0.1                                     | 1.549                     | 1794                   | 3.635      | 1.745   |

(a) C<sub>p</sub> – heat capacity; ρ – density; k – thermal conductivity.

(b) Averaged values for the properties are used here due to the condensed state of molten salt. For comparison purposes: 60% NaNO<sub>3</sub> and 40% KNO<sub>3</sub>; Melting point: 222°C; Boiling point: 704°C.

Table 7. Values of  $X_T$ , suggested operating parameters, and thermodynamic properties of heat transfer fluids

3.4 Flow characteristics of the heat transfer fluids in the transport pipeline

The heat loss of the transport pipeline is greatly influenced by the flow characteristics. The flow parameters such as flow velocity and pressure loss must be controlled in an acceptable engineering range in the pipeline. The velocity is determined by the flow rate and pipe diameter. The flow rate can be calculated from  $X_T$  and the heat load. Figure 2 shows the dependence of helium flow velocity on the heat load and pipeline diameter. It can be found that the velocity depends strongly on the pipeline diameter. Utilizing a smaller diameter pipeline can reduce the construction cost. However, a smaller pipeline diameter may lead to a higher velocity and larger pressure drop, which requires an increased pressure boosting for the pipeline transport.

To estimate the pressure drop, the following equation is adopted:

$$\frac{\Delta P}{L} = f \cdot \frac{1}{D} \cdot \frac{\rho u^2}{2} \tag{7}$$

where  $\Delta P/L$  is the pressure drop per unit length (Pa/m),  $D$  is the pipeline inside diameter,  $\rho$  is the helium density (values given in Table 7),  $u$  is the helium velocity (values given in Fig. 2),  $f$  is the friction factor determined by the Reynolds number and the pipeline inner wall roughness. Then from equations (6) and (7), the pressure loss can be calculated by:

$$\frac{\Delta P}{L} = \frac{1}{2} \left( \frac{4}{\pi} \right)^2 \frac{f}{\rho} \cdot X_T^2 \cdot D^{-5} \cdot Q_T^2 \tag{8}$$

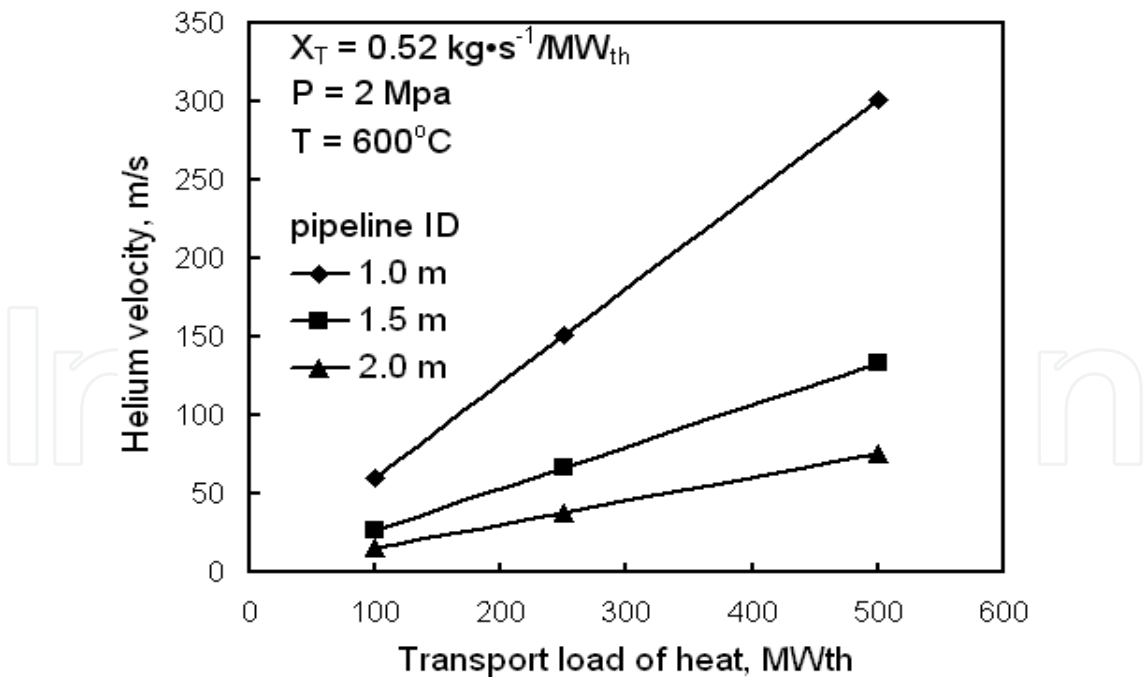


Fig. 2. Dependence of helium flow velocity on the heat load and pipeline diameter

Figure 3 shows the dependence of pressure drop on heat load and pipeline diameter. For the pipeline diameter of 1.0 m, the pressure loss may reach 500 kPa/km (5 bars/km) when the heat load is 500 MW<sub>th</sub> (about 150 tons H<sub>2</sub>/day). To pump helium 10 km away, the pressure

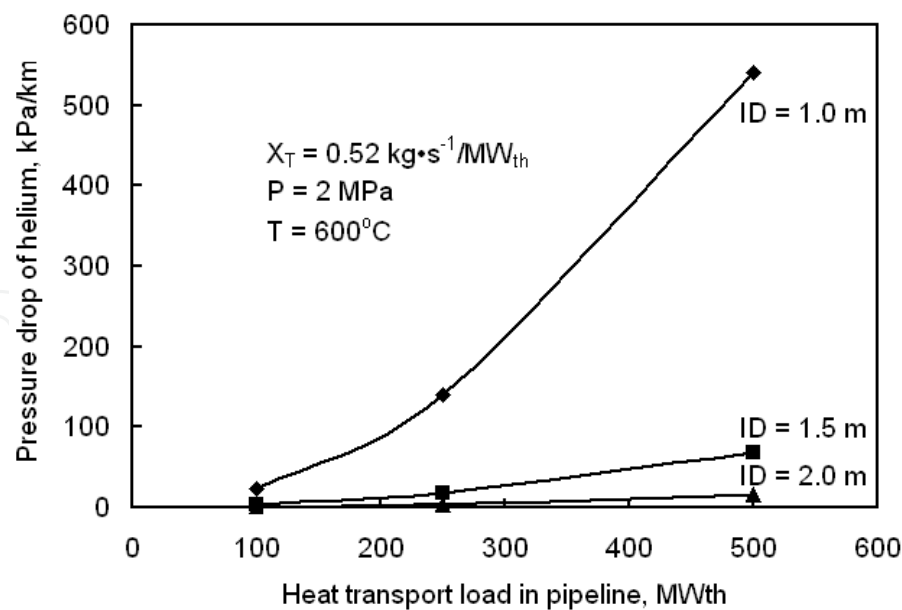


Fig. 3. Dependence of helium pressure drop on the heat load and pipeline diameter

loss is about 50 bars (5 MPa). This is a large pressure loss that may need significant compressor work. To lower the pressure loss, the pipeline diameter must be increased or multiple pipelines must be utilized.

3.5 Heat transport load and heat loss in the transport pipeline

When heat is transported by helium from a nuclear station to a hydrogen plant, it will experience heat losses. The influencing parameters include the helium flow rate, heat load, temperature, pipeline diameter, insulation, and weather conditions, among others. The heat loss is transferred from helium to the pipeline wall mostly through convection, and then through the conduction of the insulation of the pipeline, and lastly to air through convection and radiation if the pipeline is on the ground surface. If the pipeline is buried underground, the heat loss mostly goes to the soil. Since the thermal conductivity of metal is usually at least one order larger than most types of soils, the soil can also serve as insulation if the soil moisture is not significant. Due to the variations of soil types, buried depth and transport length of pipeline, the investigation of the heat loss for underground pipelines is not discussed in detail here. To simplify the evaluation, this paper will mainly examine the heat loss of the surface pipeline.

Since the pipeline is sufficiently long compared with its diameter, the axial flow effect can be neglected. The heat transfer can be approximated as a one-dimensional flow in the radial direction. The heat loss per unit length of the pipeline can be calculated with the following equation [Lienhard et al., 2008]:

$$\frac{Q}{L} = \frac{2\pi(T_{He} - T_{air})}{\frac{1}{R_i h_{convec}^{He}} + \frac{\ln(R_o / R_i)}{k_{pipe}} + \frac{\ln[(R_o + \theta) / R_o]}{k_{insu}} + \frac{1}{(h_{convec}^{air} + h_{rad})(R_o + \theta)}} \tag{9}$$

where  $Q/L$  is the heat loss per unit length,  $T_{He}$  is the average helium temperature in the pipeline,  $T_{air}$  is the air temperature varying with days and seasons,  $R_i$  and  $R_o$  are the pipeline inside and outside radius (not including the insulation),  $k_{pipe}$  is the thermal conductivity of

the pipeline material,  $\theta$  is the insulation thickness,  $h_{convec}^{He}$  and  $h_{convec}^{air}$  are the convection heat transfer coefficients of helium flow in the pipeline and wind outside the insulation, and  $h_{rad}$  is the radiation heat transfer coefficient.

To have a safe design approximation, the upper value of the thermal conductivity of insulation for a very high temperature environment (600°C) is adopted. It is also assumed that the outer surface of the insulation will be oxidized after use of some time so that the emissivity coefficient is higher than that of a well maintained condition. In addition, extreme cold weather conditions may take place occasionally. Table 8 shows the parameters of the pipeline, insulation and weather conditions for the calculation of heat losses.

| Pipeline  | Insulation  |            | Air   |            |
|---|---|------------|---|------------|
| Thermal conductivity                            | Thermal conductivity  | Emissivity | T   | Wind speed |
| 15 w/m·K  | 0.25 w/m·K  | 0.31       | -50°C   | 6.0 m/s    |
| Stainless Steel AISI 304L [Assael et al., 2003] | Ceramic fiber blanket wrapped by heavily oxidized aluminum foil [Desjarlais et al., 2002; Engineeringtoolbox, 2010] |            | Ontario, Canada [Ontario Government Data, 2010] |            |

Table 8. Parameters of pipeline, insulation and weather conditions for heat loss estimate

Figure 4 shows the estimated heat losses for the heat transport loads of 200 - 700MW<sub>th</sub>. It can be found that the heat loss can be controlled to below 2 MW<sub>th</sub>/km if the insulation thickness

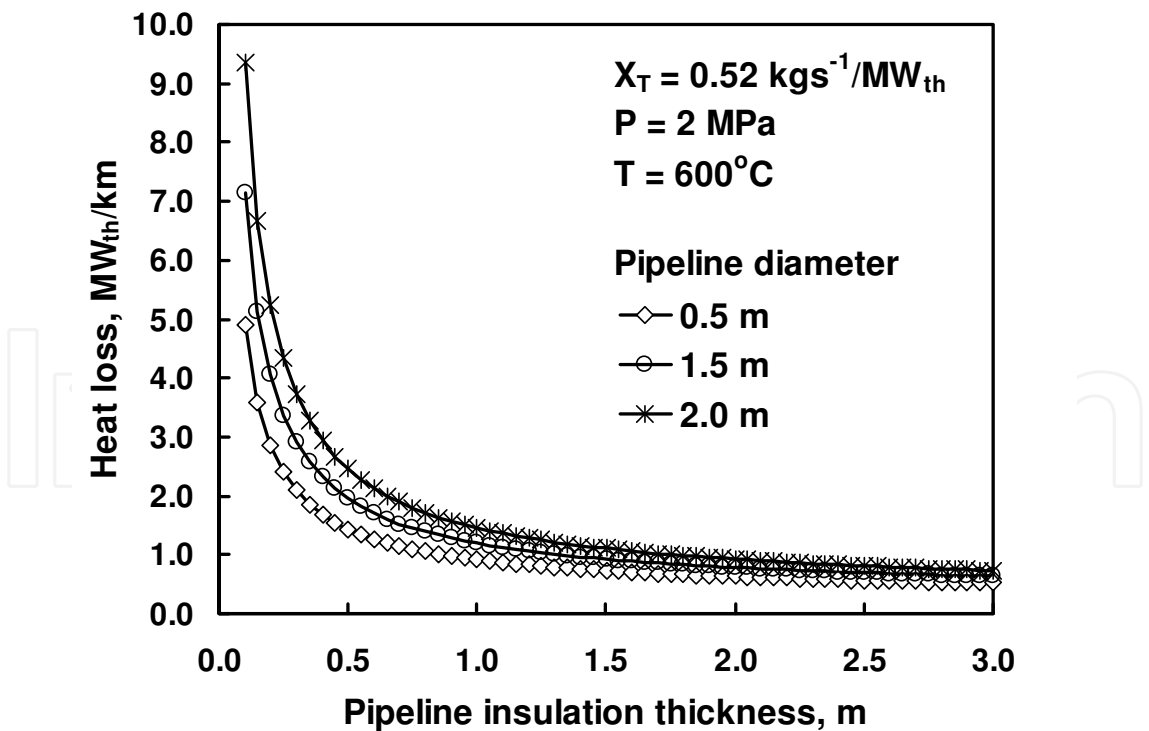


Fig. 4. Heat losses of pipeline for the heat transport loads of 200 - 700MW<sub>th</sub>

is larger than 1.0m. This suggests the key importance of the pipeline insulation. If considering both the pipeline diameter (e.g. 1.0m) and insulation thickness (1.0m), the total

diameter would be about 3.0m, which creates a barrier for animals and human activities if the pipeline is constructed on the ground surface. To bury the pipeline underground is another option. An underground pipeline will increase construction and maintenance costs. Assume the cost of insulation is much lower than the pipeline so that the insulation thickness can be constructed larger than 1.0 m. Then the heat loss of  $2.0 \text{ MW}_{\text{th}}/\text{km}$  can be considered as a typical value for the transport. When the heat load is higher, the heat loss percentage is lower. When the pipeline length is 10 km, then the heat loss is  $20 \text{ MW}_{\text{th}}$ . If the heat load is  $500 \text{ MW}_{\text{th}}$  (about 150 tonnes  $\text{H}_2/\text{day}$ ), the two-way heat loss is then about 12.5%. However, Fig. 4 also shows the limit of heat loss reduction by insulation: to increase the insulation thickness does not always have a significant heat loss reduction effect when the thickness is larger than 1.5m. Considering the heat loss through pumps and other components such as valves and expansion joints, the heat loss for a two-way transport pipeline design is assumed below 20% when the transport distance from a nuclear reactor to a hydrogen plant is within 10 km. The analysis shown in Table 6 of the former section is based on this value.

#### 4. Layout options for the integration of nuclear and hydrogen production plants

When a nuclear reactor is coupled with a hydrogen production plant, the layouts for the heat and fluid flows are important for safety and economics. The layout options depend strongly on the reactor types. Since the indirect or reheat cycle nuclear reactors have a secondary coolant or circulation that can provide heat to the heating fluid of a hydrogen plant through an intermediate heat exchanger, the integration of a hydrogen production plant with an indirect or reheat cycle nuclear reactor may provide safer and more flexible layout options. Therefore, the focus of this section will examine the direct cycle nuclear reactors, which are represented by SCWR in this chapter.

Figure 5 shows the arrangement of a supercritical water-cooled nuclear reactor (SCWR) and a hydrogen cogeneration plant with the Cu-Cl thermochemical cycle. The values of temperatures and pressures of the flowchart were calculated according to the water stream enthalpy change and expansion ratio that were reported in the past [Yamaji et al., 2005; Naidin et al., 2009]. The streamlines for the supercritical water are based on existing fossil fuel power plants that use a supercritical water turbine after changing the fossil fuel combustion chamber and supercritical water tank to SCWR [Yamaji et al., 2005; Naidin et al., 2009; Buongiorno et al., 2002]. The water stream circulation passing the lines A-B-C-D-E and A-B-F-E in Figure 5 has the typical features of a no-reheat system that uses a preheater and two types of turbines, i.e., high pressure (HP) and low pressure (LP) turbines. From the temperatures shown in Figure 5, it can be found that point A, i.e., the location downstream of the nuclear reactor but upstream of the turbines, can provide around  $100^\circ\text{C}$  of a driving temperature difference for step IV of the Cu-Cl cycle that requires  $530^\circ\text{C}$ . At this location, a bypass line of the supercritical water stream passing points A and N can be designed for heat extraction from supercritical water to the Cu-Cl cycle. An intermediate heat exchanger can be arranged on the line A-N-B to provide heat to helium that is used to heat the hydrogen cycle through the circulation of H-I-J-K-L. For step III of the Cu-Cl cycle, the temperature requirement is  $375^\circ\text{C}$ . The heat for this step can be supplied by the helium stream exiting step IV that still has a temperature higher than  $530^\circ\text{C}$  at point I. The helium stream exiting step III at point J still has a temperature higher than  $375^\circ\text{C}$ , so it can be used for step II. Since step I of the Cu-Cl cycle needs electricity for electrolysis, the electricity can

be conducted from the generator to the Cu-Cl cycle, as shown by the line passing points O and M..

As to the water stream for the power generation, there could be a number of preheaters, or the water stream circulation could be designed as a multiple reheat cycle. The details of these layouts will not be discussed in this chapter since these designs can provide multiple options for the heat extraction bypass lines and the water stream circulation layout. Also, a single reheat cycle layout, including its steam turbines and generator, is most widely employed in current BWR and PWR technologies that can be applied to SCWR so as to reduce the design complexity.

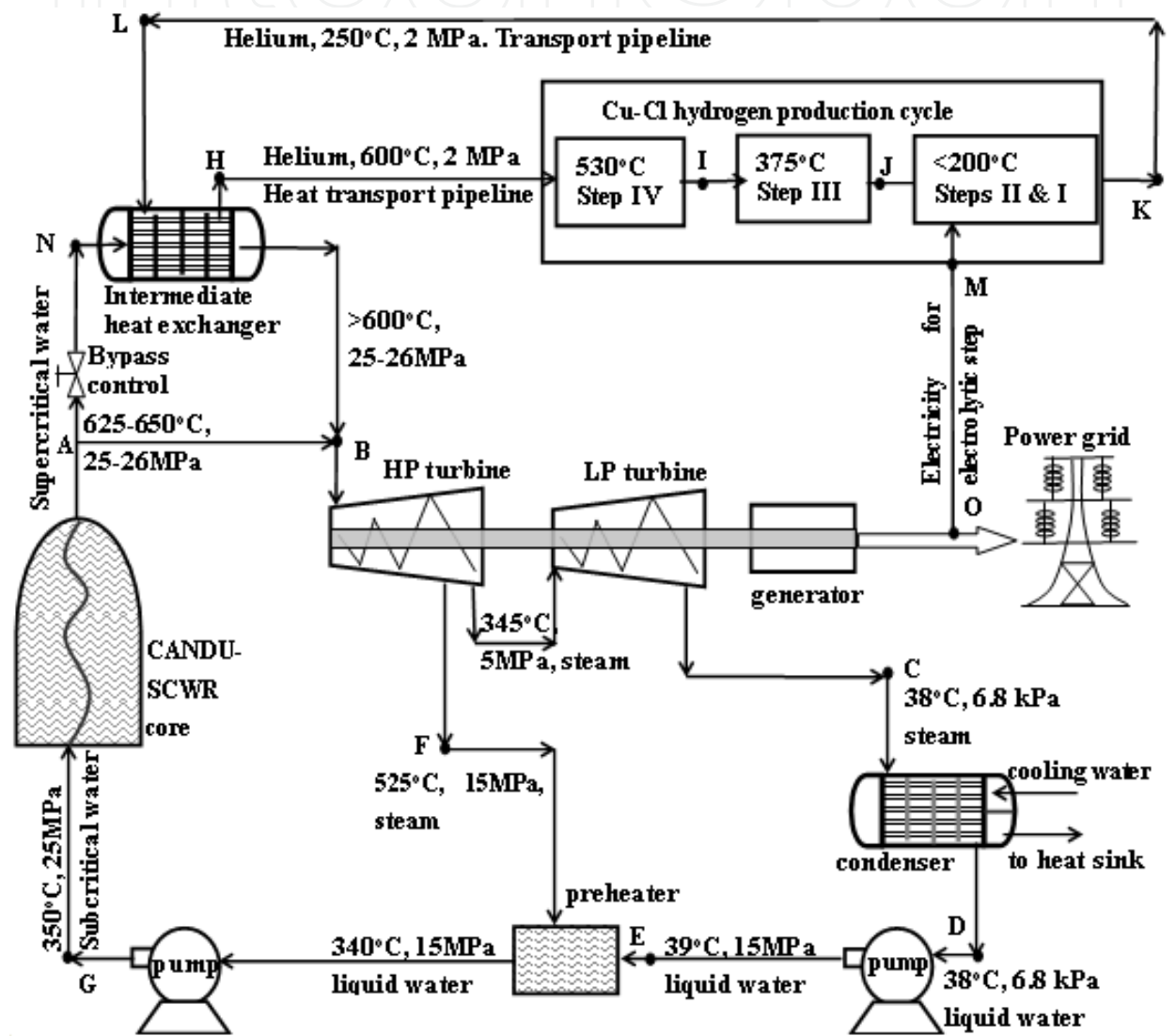


Fig. 5. Layout options for the integration of SCWR and Cu-Cl cycle (coolant passing through high pressure and low pressure turbines in series)

5. Modulation of nuclear energy output and hydrogen cogeneration scale

The demand on power varies hourly, daily, monthly and seasonally on the power grid. Figure 6 shows an actual power load profile on the power grid of a day (January 18, 2010) in

Ontario, Canada [IESO, 2010]. It can be found that the power demand varies significantly at different hours. The gap between peak and off-peak hours can even reach 70% of the base power load. Since the power grid comprises various energy sources such as nuclear, fossil fuels, hydro, solar and wind, the modulation of the power output from these sources is very

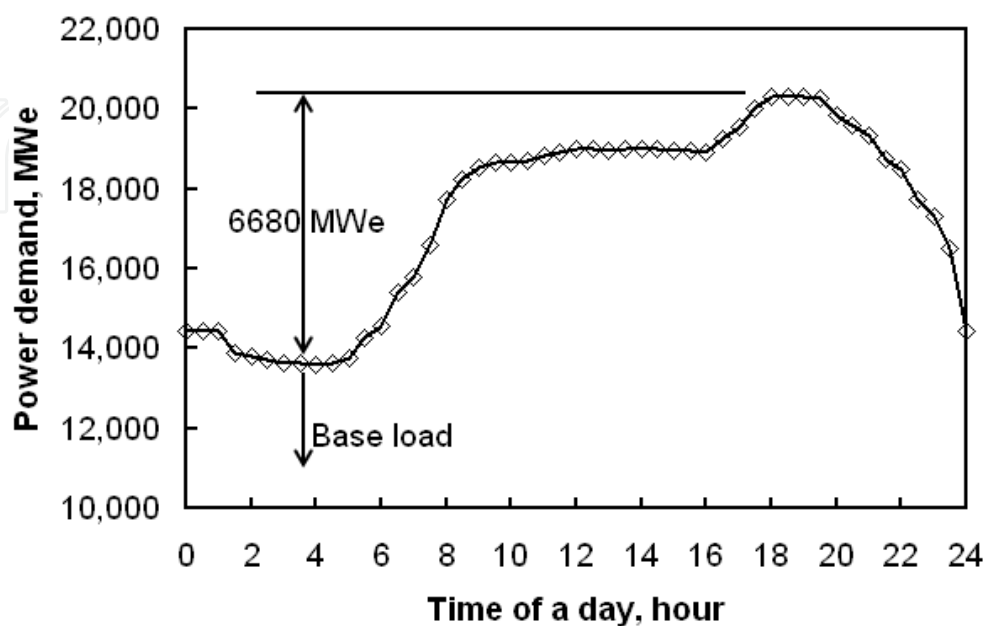


Fig. 6. Typical power load profile of a day in Ontario, Canada (January 18, 2010).

important. This means some power plants cannot operate at a constant power output. The selection of energy sources to be adjusted upward to meet the peak power demand will influence the amount of greenhouse gas emissions. To increase the nuclear power output for the peak hour demand can reduce the greenhouse gas emissions, so there are some countries employing and developing nuclear modulation technologies to adjust the power output. The modulation technologies include the adjustment of control rod insertion depth, the velocity of circulation steam, new types of grey rods, or a combination thereof [WNA , 2011; Gilbert et al., 2004]. However, the adjustment of nuclear power output may directly influence the operation of the nuclear reactor and introduce more safety issues than a constant power output, so most countries use other energy sources such as fossil fuel and hydroelectric power to follow the power demand on the grid. The percentage of nuclear power in the base load in Figure 6 is maximized to lower the portions of other energy sources. However, the base load varies monthly and seasonally, so the nuclear power plant can rarely operate at its full design capacity of power generation, except if the nuclear portion in the base load is small.

Using nuclear energy (either in the form of electricity or heat) to produce hydrogen at off-peak hours and surplus generation capacity is a promising option. As shown in Figure 7, both the heat and electricity outputs are controlled to be constant. The electricity delivered to the power grid can follow the power load profile on the grid (either fully or partly), and the rest of the electricity goes to conventional water electrolysis. This option has no requirement of modulating the heat and electricity output of the nuclear reactor, but the hydrogen production facilities must be able to accommodate the modulation of production rate.

Figure 8 shows another option that has no requirement of modulating the heat but must modulate the electricity generator to accommodate varying heat input, and at the same time

to modulate the hydrogen production rate. In both options, the total heat output from a nuclear reactor is constant, so it is anticipated to be safer than the measure of varying heat output. In comparison, option 1 is safer and more simple in principle, but the hydrogen production efficiency with water electrolysis is lower than with thermochemical cycles in option 2, which may influence the hydrogen production scale and economics.

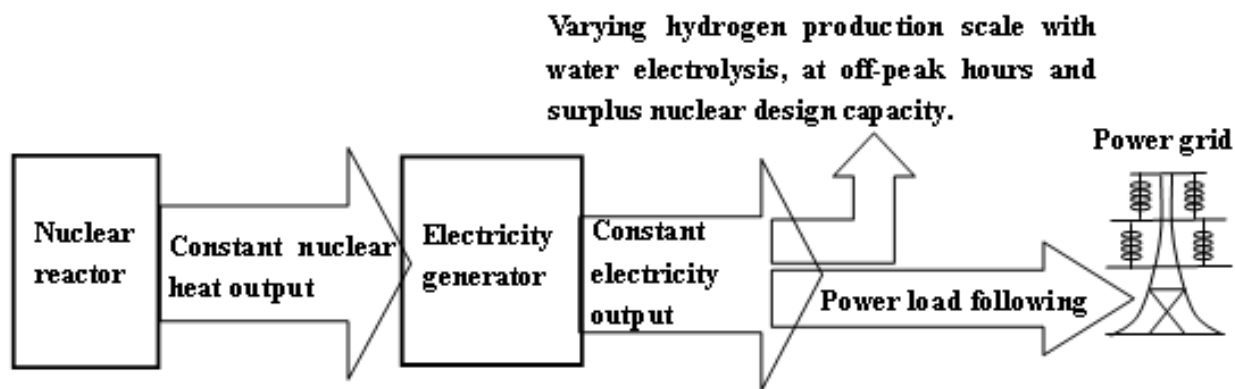


Fig. 7. No modulation of both nuclear heat and electricity with water electrolysis

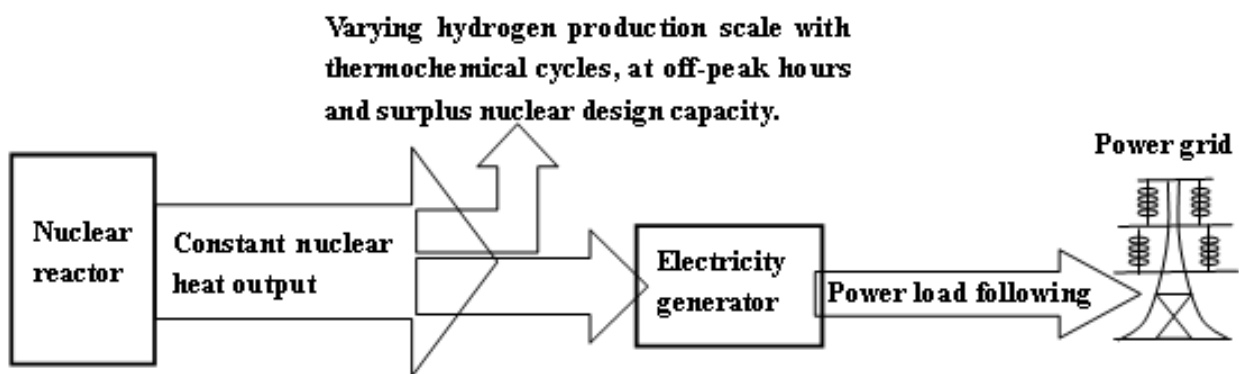


Fig. 8. No modulation of nuclear heat with thermochemical cycles

Table 9 shows the hydrogen production rate at different hours of a day. The values are calculated on the basis of the design capacity of 1,000 MWe for a Generation IV single supercritical water-cooled nuclear reactor (SCWR). The SCWR operates at its maximum capacity with cogeneration of hydrogen. The available heat for hydrogen production is the difference between the design capacity of the SCWR and the power generated that is following the power demand profile of the power grid shown in Figure 6. The heat supplied to the Cu-Cl cycle from SCWR for the thermochemical Cu-Cl cycle is assumed to have a loss of 20% within 10 km, as discussed in the former section. The data in Table 5 is used to determine the heat requirements of the Cu-Cl cycle. The overall efficiencies of water electrolysis and the Cu-Cl cycle are assumed to be 30% and 45% respectively, which suggests a smaller efficiency gap than shown in Table 2 so as to have a conservative estimate. It can be found that a single SCWR at off-peak hours and surplus design capacity can produce at least 100 tonnes of hydrogen each day. This production rate is equivalent to the production capacity of an industrial plant with steam methane reforming, which is the major technology employed today.

| Time<br>hour  | Generated power and<br>design capacity, MW <sub>e</sub> |                    | Available heat for H <sub>2</sub><br>production, MW <sub>th</sub> |  | H <sub>2</sub> production rate<br>Tonnes/day |                |
|---|---|--------------------|---|--|--|----------------|
|   | % of full<br>design<br>capacity                         | Generated<br>power | Unused<br>power<br>capacity                                       | Unused heat<br>quantity <sup>(a)</sup> | Water<br>electrolysis                        | Cu-Cl<br>cycle |
| 1-5am   | 53%   | 530                | 470   | 1044                                   | 265  | 318            |
| 5-6am   | 56%   | 560                | 440   | 844                                    | 248  | 298            |
| 6-7am   | 62%   | 620                | 380   | 978                                    | 215  | 257            |
| 7-8m  | 66%   | 660                | 340   | 756                                    | 192  | 230            |
| 8-9am   | 70%   | 700                | 304   | 676                                    | 172  | 206            |
| 9am-16pm  | 74%   | 740                | 260   | 578                                    | 147  | 176            |
| 16-17pm   | 75%   | 750                | 250   | 556                                    | 141  | 169            |
| 17-18pm   | 78%   | 780                | 220   | 489                                    | 124  | 149            |
| 18-19pm   | 80%   | 800                | 200   | 444                                    | 113  | 136            |
| 19-20pm   | 78%   | 780                | 220   | 489                                    | 124  | 149            |
| 20-21pm   | 74%   | 740                | 260   | 578                                    | 147  | 176            |
| 21-22pm   | 66%   | 660                | 340   | 756                                    | 192  | 230            |
| 22-23pm   | 60%   | 600                | 400   | 889                                    | 226  | 271            |
| 23pm-1am  | 54%   | 540                | 460   | 1022                                   | 260  | 312            |
| (a) The thermal efficiency of power generation is assumed to be 45% for SCWRs [Kirillov, 2008, Yamaji, 2005; Naidin, 2009; Buongiorno, 2002]. |   |                    |   |  |  |                |

Table 9. Hydrogen production scale and quantity with nuclear energy at various hours

6. Conclusions

This chapter examined the usage of nuclear energy for the cogeneration of electricity and hydrogen with water splitting technologies, so as to improve the economics of power plants and at the same time reduce greenhouse gas emissions. The hydrogen economy is discussed and the reduction of greenhouse gas emissions by use of nuclear generated hydrogen as a substitute of fossil fuels is quantified. The thermal efficiencies and economics of various hydrogen production methods with nuclear energy are examined. The methods include thermochemical water splitting cycles, conventional electrolysis, and high temperature electrolysis. Among these methods, thermochemical cycles have the most promisingly high efficiency and economics. It is found that the relatively high temperature requirements of

numerous thermochemical cycles are the common threshold of utilizing nuclear heat to produce hydrogen. The copper-chlorine (Cu-Cl) cycle has a minimum temperature requirement (about 530°C) that can be met by most Generation IV nuclear reactors. The temperature of a nuclear reactor should not only meet the threshold, but it should also match the heat distribution of the thermochemical cycle. Also, the nuclear reactor temperature must be high enough to offset the heat losses in the heat transport pipeline. The future studies of thermochemical hydrogen production can be conducted toward lowering the temperature requirements. An intermediate heat exchanger is suggested between the nuclear reactor and thermochemical cycle so as to minimize the mutual influence between the plants and improve the safety and operating flexibility.

Various heat transfer fluids for the heat exchange and transport pipeline were compared and evaluated. Considering the heat transport complexity in the pipeline and the importance of being chemically inert, phase change fluids and thermal oils are not suggested. Pressurized helium is a promising option for serving as the long distance heat transport fluid in the pipeline. A challenge of the heat transport in a pipeline is the pressure boosting requirement to overcome the considerable pressure losses if the pipeline diameter is smaller than one meter or the heat transport load is too large. Another challenge is the large diameter of the pipeline and thermal insulation. In order to control the two-way heat loss below 20%, the diameter must be larger than 3 meters (thermal insulation inclusive), which is a challenge for either underground or surface transport. The overall layout options for the integration of nuclear reactors and hydrogen production plants are also discussed, including the distant heat transport from nuclear reactors to a hydrogen production plant. Direct cycle nuclear reactors are discussed in more detail due to less flexibility than indirect cycle reactors.

The modulations of nuclear energy output and hydrogen cogeneration rates are also discussed in this chapter. The energy output modes of nuclear reactors include constant and variable output. Similarly, the hydrogen production scales also have two modes that are determined by the modulated heat availability of the nuclear reactors. It is concluded that a constant total heat output can be approached if the hydrogen is produced from thermochemical cycles. A constant total electricity output can also be approached with conventional water electrolysis. The constant energy output (either in the form of heat or electricity) from a nuclear reactor can provide a load following pattern that can meet the power load profile on the grid, so as to reduce the usage of fossil fuels for peak hours. The thermal energy of a single Generation IV nuclear reactor at off-peak hours and surplus design capacity are sufficient to power an industrial hydrogen plant with a thermochemical cycle or water electrolysis.

## 7. Acknowledgements

Support of this research from Atomic Energy of Canada Limited and the Ontario Research Excellence Fund is gratefully acknowledged.

## 8. References

- Assael, M. J. & Gialou, K. (2003). Measurement of the Thermal Conductivity of Stainless Steel AISI 304L up to 550 K. *International Journal of Thermophysics*, Vol. 24, pp. 1145-1153

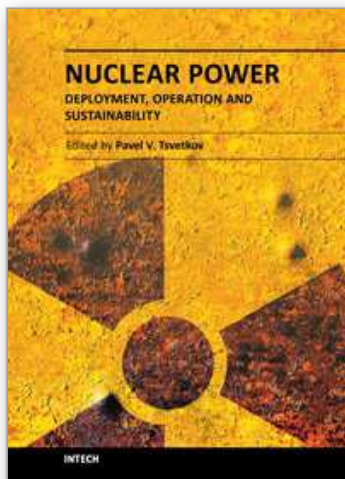
- Buongiorno, J. (2002). The Supercritical-water-cooled Reactor (SCWR). *American Nuclear Society (ANS) Winter Meeting*, Washington DC, US, November 18, 2002.
- de Jong, M; Reinders. A. H. M. E.I; Kok, J. B. W. & Westendorp, G. (2009) Optimizing a Steam-methane Reformer for Hydrogen Production. *International Journal of Hydrogen Energy*, Vol. 34, pp. 285 – 292
- Desjarlais, A. O. & Zarr, R. R. (2002) Insulation Materials. Printed in Bridgeport, NJ, US. ISBN 0-8031-2898-3. 2002, Vol. 4, pp. 122-128
- Engineeringtoolbox (2010). The Radiation Heat Transfer Emissivity Coefficient of Some Common Materials as aluminum, Brass, Glass and Many More. Available from (Accessed on Oct 4, 2010): [http://www.engineeringtoolbox.com/emissivity-coefficients-d\\_447.html](http://www.engineeringtoolbox.com/emissivity-coefficients-d_447.html)
- Forsberg, C. W. (2007). Future Hydrogen Markets for Large-scale Hydrogen Production Systems. *International Journal of Hydrogen Energy*, Vol. 32, pp. 431-439.
- Forsberg, C. W. (2003). Hydrogen, Nuclear Energy, and the Advanced High-temperature Reactor. *International Journal of Hydrogen Energy*, Vol. 28, pp.1073-1081
- Forsberg, C. (2002). Hydrogen, electricity, and nuclear power. *Nuclear news*, September 2002, pp. 30-31
- Gilbert, M. M. (2004) Renewable and Efficient Electric Power Systems. ISBN: 978-0-471-28060-6. Wiley-IEEE Press, August 11, 2004, pp. 135-148
- Government of Alberta (2008). Electricity statistics. Available from (Accessed on May 20<sup>th</sup>, 2010): <http://www.energy.alberta.ca/Electricity/682.asp>
- IEA (International Energy Agency) (2010). Hydrogen Production & Distribution. *IEA Energy Technology Essential.*, Available from (Accessed on December 20, 2010): <http://www.iea.org/techno/essentials5.pdf>
- IESO (Independent system operator) (2010). Ontario Demand on MW. Available from (Accessed on November 26, 2010): <http://www.ieso.ca/imoweb/monthsYears/monthsAhead.asp>
- Jean-Pierre Py & Capitaine, A. (2006) Hydrogen Production by High Temperature Electrolysis of Water Vapour and Nuclear Reactors. *16th World Hydrogen Energy Conference (WHEC16, 2006)*, June 13-16, Lyon, France.
- Kirillov, P. L. (2008). Supercritical Water Cooled Reactors. *Thermal Engineering*, Vol. 55, pp. 361-364
- Kreith, F & Yogi Goswami, D. (2007). Handbook of Energy Efficiency and Renewable Energy. Publisher: CRC press, ISBN: 9780849317309, ISBN 10: 0849317304, Chaper 6
- Kubo, S.; Kasahara, S.; Okuda, H; Terada, A; Tanaka, N.; Inaba, Y.; Ohashi, H.; Inagaki, Y.; Onuki, K. & Hino, R. (2004). A Pilot Test Plan of the Thermochemical Water-splitting Iodine-sulfur Process. *Nuclear Engineering and Design*, Vol. 233, pp. 355-362
- Lienhard IV, J. H.; Lienhard V, J. H. (2008) A Heat Transfer Textbook. 3<sup>rd</sup> edition, Phlogiston Press, Cambridge, Massachusetts, USA, 2008, Chapters III and IV, pp. 341-594
- Naidin, M., Mokry, S., Baig, F. & Gospodinov, Y. (2009). Thermal-Design Options for Pressure-Channel SCWRS With Cogeneration of Hydrogen. *Journal of Engineering for Gas Turbines and Power*, Vol. 131, pp. 012901-1~80

- Naterer, G.F. ; Fowler M.; Cotton J. & Gabriel K. (2008). Synergistic Roles of Off-peak Electrolysis and Thermochemical Production of Hydrogen from Nuclear Energy in Canada. *International Journal of Hydrogen Energy*, Vol. 33, pp. 6849 – 6857.
- NYSERDA (New York State Energy Research and Development Authority) (2010). Hydrogen Fact Sheet: Hydrogen Production -- Steam Methane Reforming (SMR). *Technical report - Clean Energy Initiative.*, Available from (Accessed on May 1<sup>st</sup>, 2010): <http://www.getenergysmart.org/files/hydrogeneducation/6hydrogenproductionsteammethanereforming.pdf>
- Ontario government data (2010). Available from (Accessed on Oct 4, 2010): <http://www.omafra.gov.on.ca/english/engineer/facts/03-047.htm#f13>
- Petersen, H (1970). The Properties of Helium: Density, Specific Heats, viscosity, and Thermal Conductivity at Pressures from 1 to 100 bar and from Room Temperature to about 1800 K. *Risø Report No. 224. Danish Atomic Energy Commission Research Establishment Risø*. September, 1970.
- Sadhankar, R. R.; Li, J.; Li, H.; Ryland, D. & Suppiah, S. (October 2005). Hydrogen Generation Using High-temperature Nuclear Reactors. *55th Canadian Chemical Engineering Conference*, Toronto
- Schultz, K. (2003) Thermochemical Production of Hydrogen from Solar and Nuclear Energy. Presentation to The Stanford Global Climate and Energy Project. 14 April, 2003. General Atomics, San Diego, California, US. Also available from: [http://gcep.stanford.edu/pdfs/hydrogen\\_workshop/Schultz.pdf](http://gcep.stanford.edu/pdfs/hydrogen_workshop/Schultz.pdf)
- Sivula, K.; Zboril, R.; Le Formal, F.; Robert, R.; Weidenkaff A.; Tucek, J.; Frydrych, J. & Grätzel, M. (2010). Photoelectrochemical Water Splitting with Mesoporous Hematite Prepared by a Solution-Based Colloidal Approach. *Journal of American Chemical Society*, Vol. 132, pp. 7436–7444
- Steinfeld, A. (2005). Solar Thermochemical Production of Hydrogen – A Review. *Solar Energy*. Vol. 78, pp. 603–615
- Wang, Z. L. & Naterer, G. F. (2010). Greenhouse Gas Reduction in Oil Sands Upgrading and Extraction Operations with Thermochemical Hydrogen Production. *International Journal of Hydrogen Energy*, Vol. 35, pp. 11816–11828
- Wang, Z.L.; Naterer G. F.; Gabriel, K.S.; Gravelsins, R. & Daggupati, V.N. (2010). Comparison of Sulfur-iodine and Copper-chlorine Thermochemical Hydrogen Production Cycles. *International Journal of Hydrogen*, Vol. 35, pp. 4820 – 4830
- Wang, Z. L.; Naterer, G. F.; Gabriel, K. S.; Gravelsins, R. & Daggupati, V. N. (2009). Comparison of Different Copper-chlorine Thermochemical Cycles for Hydrogen Production. *International Journal of Hydrogen Energy*, Article in Press, Vol. 34, pp. 3267–3276
- WNA (World Nuclear Association). Generation IV Nuclear Reactors. Available from (accessed on December 20, 2010) <http://www.world-nuclear.org/info/inf77.html>
- WNA (World Nuclear Association) (2011). Nuclear Power in France. Available from (Accessed on March 20, 2011): <http://www.world-nuclear.org/info/inf40.html>.

Yamaji, A.; Kamei, K.; Oka, Y. & Koshizuka, S. (2005). Improved Core Design of the High Temperature Supercritical-pressure Light Water Reactor. *Annals of Nuclear Energy*, Vol. 32, pp. 651–670

IntechOpen

IntechOpen



## **Nuclear Power - Deployment, Operation and Sustainability**

Edited by Dr. Pavel Tsvetkov

ISBN 978-953-307-474-0

Hard cover, 510 pages

**Publisher** InTech

**Published online** 09, September, 2011

**Published in print edition** September, 2011

We are fortunate to live in incredibly exciting and incredibly challenging time. Energy demands due to economic growth and increasing population must be satisfied in a sustainable manner assuring inherent safety, efficiency and no or minimized environmental impact. These considerations are among the reasons that lead to serious interest in deploying nuclear power as a sustainable energy source. At the same time, catastrophic earthquake and tsunami events in Japan resulted in the nuclear accident that forced us to rethink our approach to nuclear safety, design requirements and facilitated growing interests in advanced nuclear energy systems. This book is one in a series of books on nuclear power published by InTech. It consists of six major sections housing twenty chapters on topics from the key subject areas pertinent to successful development, deployment and operation of nuclear power systems worldwide. The book targets everyone as its potential readership groups - students, researchers and practitioners - who are interested to learn about nuclear power.

### **How to reference**

In order to correctly reference this scholarly work, feel free to copy and paste the following:

Zhaolin Wang and Greg F. Naterer (2011). Water Splitting Technologies for Hydrogen Cogeneration from Nuclear Energy, Nuclear Power - Deployment, Operation and Sustainability, Dr. Pavel Tsvetkov (Ed.), ISBN: 978-953-307-474-0, InTech, Available from: <http://www.intechopen.com/books/nuclear-power-deployment-operation-and-sustainability/water-splitting-technologies-for-hydrogen-cogeneration-from-nuclear-energy>

**INTech**  
open science | open minds

### **InTech Europe**

University Campus STeP Ri  
Slavka Krautzeka 83/A  
51000 Rijeka, Croatia  
Phone: +385 (51) 770 447  
Fax: +385 (51) 686 166  
[www.intechopen.com](http://www.intechopen.com)

### **InTech China**

Unit 405, Office Block, Hotel Equatorial Shanghai  
No.65, Yan An Road (West), Shanghai, 200040, China  
中国上海市延安西路65号上海国际贵都大饭店办公楼405单元  
Phone: +86-21-62489820  
Fax: +86-21-62489821

© 2011 The Author(s). Licensee IntechOpen. This chapter is distributed under the terms of the [Creative Commons Attribution-NonCommercial-ShareAlike-3.0 License](https://creativecommons.org/licenses/by-nc-sa/3.0/), which permits use, distribution and reproduction for non-commercial purposes, provided the original is properly cited and derivative works building on this content are distributed under the same license.

IntechOpen

IntechOpen